



# Heavy metal's pollution health risk assessment and source appraisal of groundwater and surface water in Irob catchment, Tigray, Northern Ethiopia

Haile Tadelle Abadi<sup>1,2</sup> · Tewodros Alemayehu<sup>2,3</sup> · Berihu Abadi Berhe<sup>2</sup>

Received: 12 March 2024 / Accepted: 8 July 2024 / Published online: 14 August 2024  
© The Author(s) 2024

## Abstract

Contamination of water resources by heavy metals causes health problems for humans. This study attempts to investigate the heavy metal contamination levels, health risks and sources of appraisal of groundwater and surface water in the mountain-bounded catchment and low-grade basement rock-dominated area of the Irob, Tigray. Eighteen grab water samples (13 borehole water, 2 spring water and 3 surface water) were collected and analyzed for pH, electrical conductivity, total dissolved solids and heavy metals using standard procedures. The findings were contrasted with those of the standards set by the World Health Organization and the United States Environmental Protection Agency. Integrated techniques, including indexed and statistical methods, were used to determine the contamination levels of metals, risks to human health and sources. The result shows that the pH value, electrical conductivity and total dissolved solids fluctuated between 7.4 and 7.9, 516 and 2410  $\mu\text{s}/\text{cm}$  and 396.7 mg/l and 1719 mg/l, respectively. The findings indicate that 94.4% of the water samples had levels of contamination above the critical limit for all three indices: the heavy metal evaluation index (HEI), the degree of contamination (cd) and the heavy metal pollution index. The hazard index of metals for adults and children was greater than 1. 88.9% of the water samples showed a cancer risk value above the recommended value ( $\text{CR} > 1 \times 10^{-4}$ ) for Cd and Cr for both adults and children. Multivariate statistical analyses indicate that weathering of bedrocks and partly anthropogenic influences are responsible for the metal contamination. The study concludes that some water samples sources are unfit for human consumption that can pose health risks over time. Therefore, it is recommended to treat contaminated water sources to protect and sustain public health.

**Keywords** Heavy metal contamination · Pollution indices · Human health risk · Multivariate statistical analysis · Irob catchment

## Introduction

Water is the key and important basic needs of natural resources to ensure the sustainability of human life. For the survival of human life, all people have access to safe

and adequate and drinking water (WHO 2022). However, according to UNICEF (2019), 2.2 billion people worldwide have no access to hygienic water for drinking. Particularly in dry or semiarid areas, groundwater is a highly significant source of water for industrial, agricultural and residential uses (Wang et al. 2020). Groundwater is usually considered cleaner water than surface water because it naturally filters pollutants through the soil when the water enters the groundwater (Edokpayi et al. 2018). Nonetheless, groundwater can be contaminated by many pollutants, which can be produced by geogenic processes or human activities (Li et al. 2021). Among pollutants, heavy metals pose the greatest threat to the quality of water resources and are toxic even in low concentrations (Egbueri and Unigwe 2020). The main causes of heavy metals in water are geogenic processes like volcanism, ion exchange,

✉ Berihu Abadi Berhe  
berhag2000@gmail.com

<sup>1</sup> Department of Geology, Faculty of Mines, Axum University, Axum, Tigray, Ethiopia

<sup>2</sup> School of Earth Sciences, College of Natural and Computational Sciences, Mekelle University, Mekelle, Tigray, Ethiopia

<sup>3</sup> J.J Pickle Research Campus, Jackson School of Geosciences University of Texas at Austin, Bldg.13010100 Burnet Rd, Austin, USA

weathering and dissolution of rocks and soils and the breakdown of parent material and atmospheric materials (Wang et al. 2022). Some of the most prevalent anthropogenic activities that raise the concentration of heavy metals in water resources are mining, industry, agriculture, solid and liquid household waste disposal (Ahmad et al. 2020).

The human body needs some heavy metals in small amounts, for example, Pb in human body is allowed in the range of 20–280 µg/day for adults and 10–271 µg/day for children, Cd also needed in the range of 15–50 µg/day for adults and 2–25 µg/day for children, Zn 15 µg/day (US EPA 1998). Besides, Co (0.2 mg/l for adult and 0.001 mg/day for children), Cu (1.5–3 mg/day for adult and 1 mg/day for children), Fe (10–20 mg/day for adult and 7 mg/day for children), Mn (2–5 mg/day for adult and 1.3 mg/day for children) is allowed (Virag & Gergely 2016). However, excessive consumption is harmful to health (Xiao et al. 2019). The health consequences of water contaminated by heavy metals are long-term. For this reason, many researchers are interested in assessing the amount of water contamination by heavy metals. Studies in India report that groundwater pollution by heavy metals has health consequences (Ahmed et al. 2022). Groundwater contamination by heavy metals has also been reported in China to have both carcinogenic and noncarcinogenic effects on human health (Tony et al. 2021). Another study from Iran and Pakistan also showed that groundwater contaminated with heavy metals harms the health of humans (Yousef et al. 2018). Heavy metals such as Pb, Cr, Cd, Co, Ni, Cu, Mn, Fe and Zn have recently attracted great attention from researchers because they cause health problems (WHO 2022). Numerous studies have been carried out globally to evaluate the degree of heavy metal contamination in water resources. Among heavy metals, Pb, Cd, Cr, Ni, Fe, Cu, Co, Mn and Zn are found throughout the earth's crust and are more toxic than other heavy metals (Jamshaid et al. 2018).

Numerous extensively developed numerical and statistical models have been effectively employed for the assessment of water quality and the source evaluation of water elements. These methods include heavy metal pollution index, heavy metal evaluation index, contamination degree, correlation analysis, principal component analysis and hierarchical cluster analysis (Ren et al. 2021). Heavy metal pollution index is an evaluation technique that shows the cumulative effect of individual heavy metals on overall water quality (Mohan et al. 1996), whereas the heavy metal evaluation index is defined as it is the total ratio of each heavy metals concentration to the maximum allowable amount determined by regulatory standards (Edet & Offiong 2002). The total of the contamination factors for each heavy metal present in the sample determines the degree of heavy metal contamination (Hakanson 1980).

In Ethiopia, the contamination level of heavy metals and other chemicals in groundwater and surface water have been determined by various researchers such as Teym et al. (2021), Melaku et al. (2004), Kebede et al. (2012), Aschale et al. (2011) and others. Based on their findings, the researchers reported that Cr, Mn, Co, Ni, Cd and Pb in rivers and groundwater sources from many parts of Ethiopia are above the World Health Organization recommended limit. Besides, researchers suggested that the groundwater resources in many regions of Ethiopia are contaminated due to ineffective management of liquid and solid wastes that are discharged to surface water and then the contaminated surface water infiltrate to groundwater (Alemu et al. 2022; Tabor et al. 2011; Kawo & Karuppanan 2018). In the Tigray region, many researchers have conducted research regarding heavy metal concentrations in water resources. These include Beheemalingswara and Nata (2009), Mebrahtu and Zerabruk (2011), Hayelom and Geregziabher (2015) and Shifare and Seyoum (2012). During their investigation, they found that Fe, Mn, Co, Cd, Pb, Cu, Ni and Zn are above the permissible limit set by the WHO. Many researchers reported base metal mineralization in shear zones, faults, joints and fractures as disseminated vein fill in low-grade basement rocks in several parts of Tigray (Beheemalingswara and Nata 2009; Siraj 2022).

The present study, Irob catchment, is characterized by a semiarid climate, low-grade basement rock-dominated mountainous region. The people in the study area do not have an adequate water supply, and they rely on groundwater resources and partly on surface water for household purposes. History of research in the study area revealed that groundwater and surface water resources have a higher concentration of Pb, Cd and Co, which is above the WHO permissible threshold and thus unsuitable for domestic and agricultural purposes (Shifare and Syium 2012; Hayelom and Geregziabher 2015).

Thus, this study's main objective was to assess the levels of heavy metal contamination, health risks and their sources using integrated methods of heavy metal pollution index (HPI), heavy metal evaluation index (HEI), degree of contamination (Cd) and multivariate statistical tools such as hierarchical cluster analysis (HCA), principal component analysis (PCA) and correlation matrix. It will give a detailed explanation of the main sources of pollution and support water management in the Irob area to combat further contamination of groundwater resources.

## Materials and methods

### Description of the study area

The investigation was carried out in the semiarid mountainous region of northern Ethiopia in the Tigray regional state,

located approximately 167 km from the regional capital Mekelle, in the Irob Woreda (Fig. 1). The Irob catchment is located in the eastern zone of Tigray, geographically between longitudes 558,347–568,852 mE and latitudes 1,597,324–1,610,611 mN. Irob borders Eritrea to the north and Afar to the east. The area's drainage is characterized by mountain ranges, and the streams in the area are part of the tributaries of the Endeli River, which originates in Eritrea and flows into the Afar region. The altitude of the region ranges from 1492 to 2866 m above mean sea level, the gradient is more than 45°. The climate of the region is characterized by arid to semiarid conditions with a long dry summer and a short rainy season in winter. The mean annual rainfall and temperature of the study area are 392 mm and 15.7 °C, respectively. The rainy season lasts only from June to September.

### Geology and geological setting

Low-grade metavolcanic to metasedimentary rock sequences, which are part of the Tambien and Tsaliet groups of the Neoproterozoic Pan-African Arabian-Nubian Shield, determine the geology of northern Ethiopia (Alene et al. 2006; Hagos et al. 2020). Syn- and post-tectonic granitoids have intruded these rocks (Gebreyohannes 2014). The

Arabian-Nubian Shield contains a variety of VMS deposits (Barrie et al. 2016).

The geology of the study area comprises rocks ranging in age from Quaternary deposits to Precambrian basements. Plutonic, metavolcanic/clast, metasedimentary rocks are the key rock types observed in the area (Fig. 2). Metavolcanic rock of the area is characterized by the intercalations of metarhyolites, metaagglomerates, tufaceous slate and metabasalts. Gradational contact with metasediments and alteration developments such as kaolinization and epidotization were noted within this rock type. Cubic structure of altered pyrite crystals was observed with this rock type.

Rocks of welded tuff, metabreccia and metaagglomerate form the metavolcanic clast. The size, shape and chemical composition of clasts vary considerably. This kind of rock is distinguished by its formation of a steep topography and the rock composition that varies from felsic to mafic.

Slate, phyllite, metalimestone and dolomite intercalation characterize the metasedimentary rock. Slate and phyllite rocks exhibit significant foliation. The colors of these rocks vary and are brown, dark gray and light gray. Altered pyrite crystals were observed in this rock type. In addition, malachite staining was observed with the metasedimentary rock particularly with the metalimestone rock type.

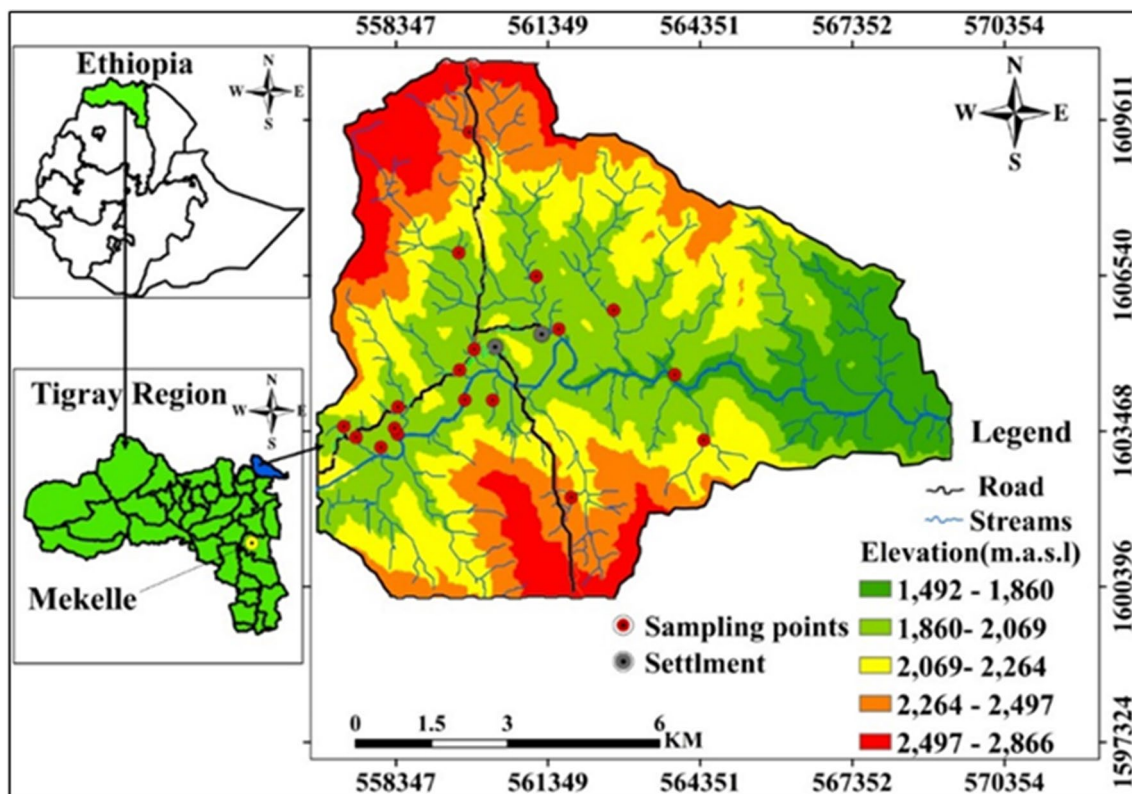


**Fig. 1** Location map of the study area: the map includes surface drainage, settlement, physiography, water sampling points and road

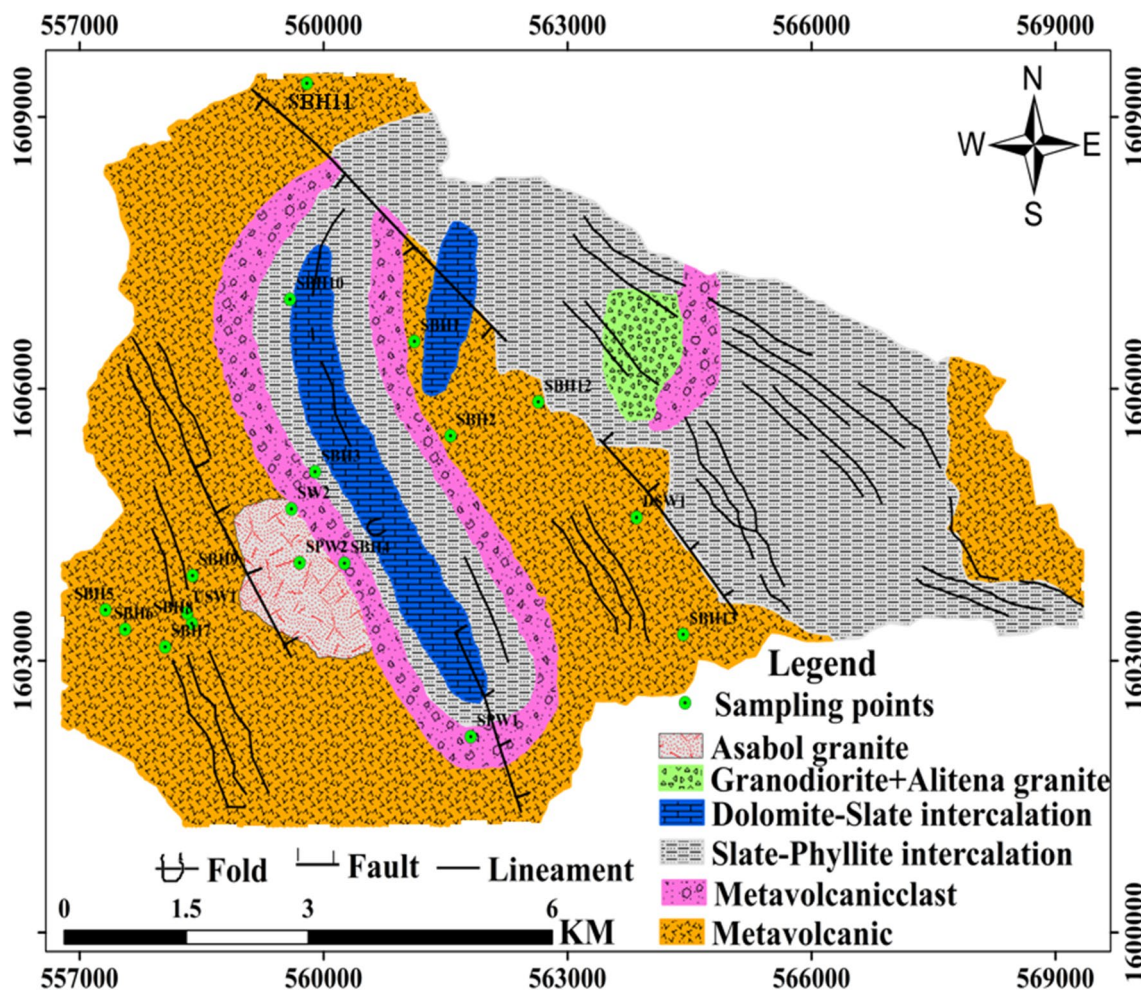


Fig. 2 Geological and structural map of the study area. The structures exhibiting different lineaments fault and fold

The basement rocks in the study area are intruded by granite dykes/sills. Granite with high peaks of ridges oriented east west with areal coverage of nearly 3 km<sup>2</sup> was noticed. In some places, the granite has a coarse-grained, gray color. In contrast, the granite in the western part has a medium-coarse grain size, a feldspar composition and pink color. The granitoid body has undergone kaolinization, which exhibits white powdery alteration along contact with metavolcanic rocks in a northeastern part of the study area. A normal fault was identified in the study area, dividing the granite into two sections.

The Quaternary sediments which make up a small part of the study area and are exposed on river bank sides and flood plains were noticed in the area. These deposits were resulted from weathering of the surrounding rocks subsequent erosion.

The geology, geomorphology and tectonic activities influence the hydrogeological system of the study area (Haile et al. 2024). Shallow weathered metavolcanic/clast, metasediment and Quaternary alluvial aquifers are

the main units for the occurrence of groundwater in the study area.

### Water sampling and sample analysis

Eighteen (18) water samples (13 borehole water, 2 spring water and 3 surface water) were collected using grab sampling technique during the dry season in March 2021 following the APHA standard procedure (2017) for sampling, preservation, transportation and analysis. Sampling included (2 spring water, 13 borehole water and 3 surface water) samples and was collected at a depth of 5–60 m for groundwater.

To make the samples representative of different geological units, geomorphology, water flow direction, accessibility, depth and land use characteristics, as well as functional and inactive wells were considered. Before sampling was carried out at the taps, the well water was pumped out for a sufficient period to clean suspended solids. The water sample from the river was collected 10 cm below the water surface following the standard procedure

prescribed by APHA (2017). To collect water samples for heavy metals, 500 ml double-cap high-density polyethylene (HDPE) storage bottles were used, which were thoroughly rinsed with nitric acid followed by distilled water. The sampling bottles were washed twice with the sample to be examined and collected at the time of sampling. The water sample was filtered in situ with the help of 0.45 μm syringe and preserved with 1 ml of nitric acid (HNO<sub>3</sub>) to avoid any precipitation. The pH and electrical conductivity (EC) were measured on site using a portable pH meter, model HANNA HI9913. Total dissolved solids was also calculated from electrical conductivity (EC) using a conversion factor of 0.64 (Brown et al. 1970). The atomic absorption spectrometer (AAS) was used to analyze the nine selected heavy metals (Fe, Mn, Co, Pb, Ni, Cu, Cd, Cr and Zn) at the geochemical laboratory analysis of Mekelle University.

The reliability of heavy metal analysis was ensured through the use of standard operating procedures, standard calibration and reagent blind analysis. Table 1 displays the heavy metals calibration curves and to check precision, a sample was randomly selected and analyzed three times. Finally, the triplicate readings for each sample were averaged. The accuracy of the analysis results is approximately ≤ 5% (Table 2).

### Method of indexing heavy metal contamination

The heavy metal pollution index (HPI), the heavy metal evaluation index (HEI) and the degree of contamination (Cd) were used to assess water suitability for drinking purposes.

#### Heavy metal pollution index (HPI)

The HPI method was used to determine the cumulative influence of individual heavy metals on overall water quality. HPI is an effective tool for assessing drinking water quality (Kumar et al. 2020; Dey et al. 2021). HPI is determined using Eq. (1). The weighted arithmetic index was used to calculate the HPI.

$$HPI = \frac{\sum_{i=1}^n WiQi}{\sum_{i=1}^n Wi} \tag{1}$$

Unit weight (Wi) is the reciprocal of Si, and Si is the WHO recommended maximum permissible value for water supply in μg/l (Kumar et al. 2020; Chiamsathit et al. 2020)

$$Wi = \frac{1}{Si} \tag{2}$$

Qi represents the *i*th parameter subindex and is computed using Eq. (3) (Biswas et al. 2017).

$$Qi = \frac{Vi}{Si} \times 100 \tag{3}$$

**Table 1** Instrument working conditions for the analysis of heavy metals

Parameters	Cd	Cr	Fe	Mn	Cu	Co	Zn	Ni	Pb
Wavelength (nm)	228.8	357.9	248.3	275.9	324	240.7	213.9	232	217
Silt width (nm)	0.5	0.2	0.2	0.2	0.5	0.2	1	0.2	1
Lamp current (mA)	10	15	5	10	15	10	10	10	12
Fuel	C2H2	C2H2	C2H2	C2H2	C2H2	C2H2	C2H2	C2H2	C2H2
Support	O2	O2	O2	O2	O2	O2	O2	O2	O2
Detection limit	0.0002	0.001	0.01	0.003	0.03	0.0005	0.0005	0.0005	0.005

**Table 2** Analysis of triplicate randomly selected sample (SBH5) coefficient of variances (CV %)

Metal	Concentration (mg/l)			Mean	SD	CV (%)
	Reading 1	Reading 2	Reading 3			
Cd	0.0264	0.024	0.0236	0.024	0.0015	6.0
Cr	0.037	0.033	0.035	0.035	0.002	5.71
Fe	2.51	2.48	2.54	2.51	0.03	1.19
Mn	0.61	0.58	0.63	0.601	0.0251	4.14
Cu	1.218	1.203	1.3	1.24	0.052	4.2
Co	0.064	0.06	0.065	0.063	0.00264	4.19
Zn	0.85	0.91	0.84	0.86	0.0378	4.36
Ni	0.813	0.74	0.815	0.789	0.0427	5.41
Pb	0.0515	0.052	0.056	0.054	0.00246	4.63

$V_i$  represents the measured concentration in  $\mu\text{g/l}$ . Heavy metal pollution index  $> 100$  represents high-risk water that cannot be used for drinking, whereas  $\text{HPI} < 100$  denotes low risk (Khelifaoui et al. 2022)

### Heavy metal evaluation index (HEI)

In addition to the HPI, the HEI approach was used to determine the pollution status of water bodies related to heavy metals. The HEI is a technique that, like the HPI, can be employed as an indicator of overall level of heavy metal contamination in water (Edet and Offiong 2002). The following formula Eq. 4 was used to calculate the HEI:

$$\text{HEI} = \sum_{i=1}^n \frac{H_C}{H_{\text{MAC}}} \quad (4)$$

where  $H_C$  represents the monitored value for the  $i$ th parameter and  $H_{\text{MAC}}$  represents the maximum acceptable limit set by the WHO. HEI has three classifications as described by Wagh et al (2018): low ( $\text{HEI} < 10$ ), medium ( $10 < \text{HEI} < 20$ ) and high ( $\text{HEI} > 20$ ).

### Degree of contamination ( $C_d$ )

The overall impact of heavy metals on the quality of water can also be determined based on the degree of contamination. This index method is very useful to summarize the cumulative effect of metals on the quality of water (Prasana et al. 2012). The mathematical formula used to determine the  $C_d$  was:

$$C_d = \sum_{i=1}^n C_{f_i} \quad (5)$$

$$C_{f_i} = \frac{CA_i}{CN_i} - 1 \quad (6)$$

where  $C_{f_i}$  represents factor of contamination for the  $i$ th parameter,  $CA_i$  is the observed concentration for the  $i$ th parameter and  $CN_i$  indicates the maximum acceptable limit. The  $C_d$  can be divided into three categories according to Edet and Offiong (2002): low if  $C_d$  less than 1), medium if  $C_d$  is between 1 and 3 and high if  $C_d$  is greater than 3.

## Human health risk assessment

### Noncarcinogenic health risk assessment

The noncarcinogenic risks of consuming water contaminated with heavy metals in adults and children have been classified by many authors (Ganiyu et al. 2021). The chronic daily intake (CDI), hazard quotient (HQ) and hazard index (HI)

**Table 3** Parameters used as input to evaluate CDI values (USEPA IRIS, 2011)

Factors	Symbol	Units	Adult	Children
Exposure frequency	EF	Days/year	365	365
Exposure duration	ED	Years	70	10
Average time	AT	(ED $\times$ 365)Days	25,550	3650
Body weight	BW	Kg	60.0	15.0
Ingestion rate	IR	L/day	2.0	1.0

**Table 4** Oral reference dose (RFD) and slope factor (SF) of heavy metals (USEPA IRIS 2011)

S/n.	Metals	Oral RFD (mg/kg/day)	Oral CSF (mg/kg/day)
1	Cd	$5 \times 10^{-4}$	0.38
2	Cr	1.5	0.5
3	Cu	$4 \times 10^{-2}$	n.d
4	Pb	$3.6 \times 10^{-4}$	0.0085
5	Zn	0.3	n.d
6	Ni	$2 \times 10^{-2}$	1.7
7	Fe	$7 \times 10^{-1}$	n.d
8	Mn	$1.4 \times 10^{-1}$	n.d
9	Co	$3 \times 10^{-4}$	n.d

of heavy metals in drinking water bodies were determined using the Eqs. 7, 8 and 9 and Tables 3 and 4.

Using guidelines proposed by the USEPA IRIS (2011), the CDI of heavy metals was calculated for children and adults as follows:

$$\text{CDI}_{\text{ing}} = \frac{C_w \times \text{IR} \times \text{EF} \times \text{ED}}{\text{BW} \times \text{AT}} \quad (7)$$

where CDI is the chronic daily intake of heavy metals (mg/kg/day) from drinking water;  $C_w$  represents the metal concentration (mg/l); IR denotes the daily water intake rate (l/day); EF denotes exposure frequency (days/year); ED represents the duration of exposure (years), BW represents the body weight (kg), AT represents the mean exposure time. The parameters used as input to evaluate the CDI are listed in Tables 3 and 4:

$$\text{HQ}_{\text{ing}} = \frac{\text{CDI}}{\text{RFD}} \quad (8)$$

$\text{HQ}_{\text{ing}}$  is the hazard quotient index by ingestion, CDI is the daily intake of heavy metals by ingestion in (mg/kg/day) and RFD is the daily reference dose of ingestion (mg/kg/day) of each element that an individual allows to consume. Heavy metals continue to be absorbed over a longer period of time without any harmful effects occurring.

$$HI = \sum_{i=1}^n HQ \quad (9)$$

The hazard quotient (HQ) is used to get the result for the noncarcinogenic risk assessment. The HQ values for each water sample are summed to obtain HI. When the HI value is  $> 1$ , heavy metals can cause adverse effects on human health, while a value  $< 1$  indicates that the effects are minor (Wei et al. 2023). In addition to this categorization, many authors divide HI into several categories. Negligible risk level if  $HI < 0.1$ , low-risk level if  $0.1 \leq HI < 1$ , medium-risk level if  $1 \leq HI < 4$  and high-risk level if  $HI \geq 4$  (Egbueri 2020).

### Carcinogenic health risk assessment (CR)

Carcinogenic risk (CR) is the risk of a person who gets cancer because of lifetime intake of heavy metals (USEPA 2011). The probability of developing cancer due to heavy metal intake during a given lifetime exposure level is determined by the following mathematical formula:

$$\text{Cancer risk (CR)} = \text{CDI} \times \text{CSF} \quad (10)$$

CSF represents cancer slope factor (mg/kg/day). A CR value  $< 10^{-6}$  indicates no carcinogenic risk, however, a value of  $CR > 10^{-4}$  indicates a higher chance of getting cancer. If the risk value is between  $10^{-6}$  and  $10^{-4}$  represents an acceptable risk (USEPA 2011). The oral reference dose (RFD) and slope factor of heavy metal value are shown in Table 4.

### Statistical analysis

In addition to descriptive statistics and multivariate statistical analyses, the data sets were analyzed using principal component analysis (PCA), cluster analysis (CA) and Pearson correlation. The strength of the intermetallic relationships was assessed using a Pearson correlation coefficient matrix. PCA has been applied to find the most common of heavy metal sources using Varimax normalized rotation. Bartlett sphericity and Kaiser–Meyer–Olkin (KMO) tests were applied to assess the data set's appropriateness for PCA. To find multivariate similarities, agglomerative hierarchical cluster analysis was used with Ward's method and squared Euclidean distance as the criterion. The IBM Statistical Package for Social Science (SPSS) v.20 statistical database was employed for all statistical analyses.

## Results and discussion

### Heavy metal contamination

The descriptive statistical analysis of three physicochemical parameters and nine heavy metals is displayed in Table 5 and compared with the WHO (2022) and USEPA (2018) guidelines.

The pH value measured in the study area was close to alkaline water and was between 7.4 and 7.9 with a mean of 7.7. All water samples are within the WHO and USEPA permissible range (6.5–8.5) (Table 5).

The range of electrical conductivity (EC) measured in the water samples was between 516 and 2410  $\mu\text{s}/\text{cm}$  (Table 5). Although there are no health-based guidelines for EC, it may have an impact on water acceptability at concentrations above 1500 ( $\mu\text{s}/\text{cm}$ ) (WHO 2022). Values above 1500  $\mu\text{s}/\text{cm}$  were found in 38.9% of the water samples.

The range of total dissolved solids varies between 396.7 mg/l and 1719 mg/l (Table 5). The WHO does not set health guidelines for TDS, but a TDS concentration above 1000 mg/l may affect the acceptability of water for drinking. 46.6% of the water samples have TDS values above the standard.

The range of Fe concentration measured was between 0.54 mg/l and 3.24 mg/l, with a mean of 1.82 mg/l (Table 5). Although the WHO (2022) has not established health-based guidelines for iron, water with an iron concentration of more than 0.3 mg/l may not be suitable for household use. 83.3% of water samples were above the WHO acceptance limit for domestic use, and all water samples were above the USEPA guideline (2018) (Table 5). Higher Fe concentrations were measured in samples collected from areas where metavolcanic/clastic rocks predominate. This shows that the source of Fe in the water sources in the study area is the Fe-containing minerals contained in this rock type. Predominantly modified pyrite crystals with a cubic structure were found in these rock types. Therefore, the Fe source could lie in the dissolution of iron sulfide minerals.

The Mn content was measured between 0.132 mg/l and 1.47 mg/l, with a mean of 0.655 mg/l (Fig. 3). The result shows that all water samples are above the permissible levels (0.08 mg/l) and (0.05 mg/l) set by the WHO (2022) and USEPA (2018), respectively (Table 5). A higher Mn concentration was measured in areas where metavolcanic/clastic rocks are predominantly present. This indicates that weathering of Mn-bearing minerals in these rock types could be the source of Mn (Beheemalingswara and Nata 2009).

The Co concentration was measured between 0.023 mg/l and 0.19 mg/l, with a mean of 0.06 mg/l

**Table 5** Descriptive statics of physicochemical parameters and heavy metals (N= 18)

Parameters (mg/l)	Min	Max	Mean	SD	Variance	WHO (2022)	USEPA (2018)	Samples exceed WHO (%)	Samples exceed USEPA (%)
pH	7.36	7.92	7.648	.1428	.020	6.5–8.5	6.5–8.5	0	0
EC( $\mu$ s/cm)	516	2410	1334	570	3257	NGL <sup>*a</sup>	NM*	–	–
Fe	.540	3.24	1.82	.837	.701	NGL <sup>*b</sup>	0.3	–	100
Mn	.132	1.47	.655	.383	.147	0.08	0.05	100	100
Co	.023	.19	.060	.038	.001	NM*	0.1	–	5.6
Cu	.407	2.56	1.47	.677	.459	2	1.3	22.2	55.5
Cd	.001	.145	.041	.039	.002	0.003	0.005	88.8	83.3
Pb	.003	.078	.044	.022	.001	0.01	0.015	88.9	88.9
Cr	.001	.08	.035	.024	.001	0.05	0.1	22.2	0
Zn	.538	1.18	.786	.182	.033	4	5	0	0
Ni	.012	1.04	.449	.374	.141	0.07	0.1	61.1	50

NM not mentioned, SD standard deviation

<sup>a</sup>NGL=No health-based guideline but may affect water acceptability at concentrations above 1500( $\mu$ s/cm),

<sup>b</sup>NGL=There is no health-based guidelines established by the WHO but may affect water acceptability at concentrations above 0.3 mg/l

**Fig. 3** Concentration value of heavy metals in water sources showing higher values of Fe, Cu, Zn and Ni compared to the other heavy metals

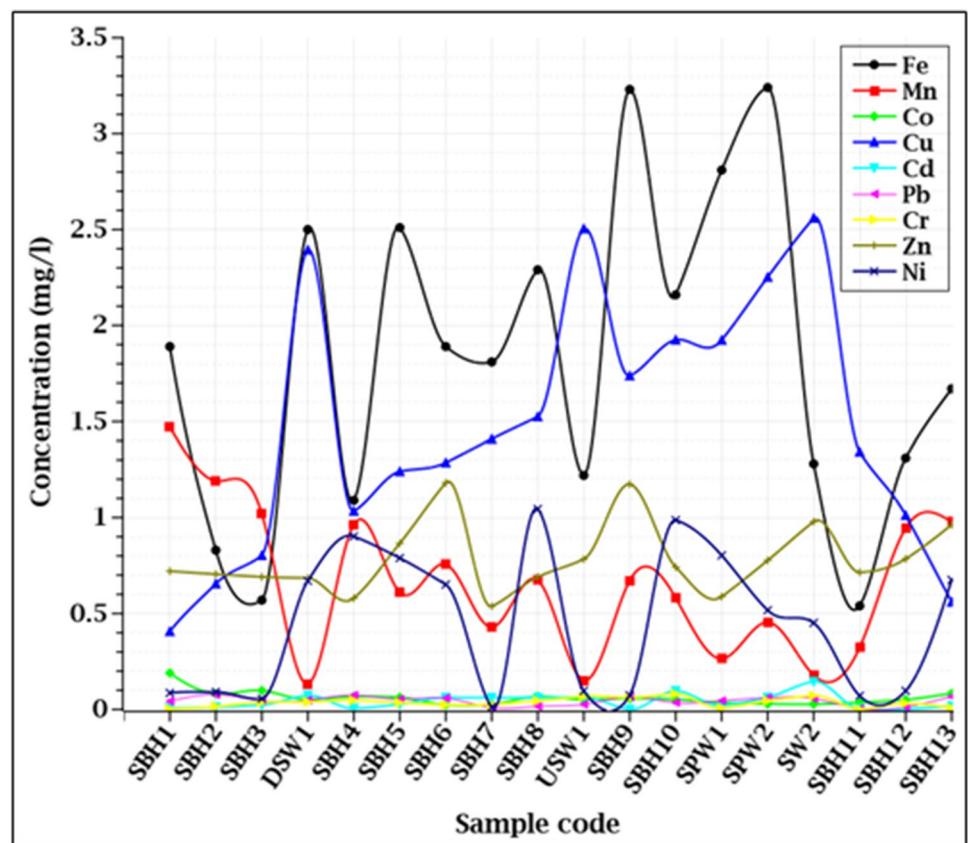


(Fig. 3). The WHO (2022) does not set an acceptable limit for cobalt, but 5.6% of water samples exceed the USEPA limit (0.1 mg/l) (Table 5).

The concentration of Cu in this study was measured between 0.047 and 2.56 mg/l, with a mean of 1.47 mg/l

(Fig. 3). 22.2% of water samples exceed the acceptable limit (2 mg/l) set by the WHO (2022) and 55.5% exceed the limit set by USEPA (2018) (Table 5). The source of Cu in the study area could be the transformation of copper sulfide minerals into copper carbonate minerals within



the carbonate rocks. This is supported by the abundance of malachite coloration ( $\text{Cu}_2\text{CO}_3(\text{OH})_2$ ) in the study area in some highly altered rocks, mainly in the metasedimentary rocks of metalimestone and metadolomite units. Base metal mineralization in the shear zone, faults, joints and fractures as disseminated vein fill in low-grade basement rocks can be the source of VMS deposits (Beheemalingswara and Nata 2009; Siraj 2022).

The Cd concentration was measured between 0.001 mg/l and 0.145 mg/l, with a mean of 0.041 mg/l (Fig. 3) and 88.8% of the water samples exceeded the acceptable limit set by the WHO (2022) (0.003 mg/l) (Table 5). Higher levels of Cd were measured in surface water near the town of Dowhan. Cadmium is recognized as the heavy metal of greatest environmental concern due to its harmful effects from prolonged use of phosphate fertilizers (Fabián et al. 2013; Abraham et al. 2024).

This higher Cd content in surface water could be due to anthropogenic Cd sources. There is no well-managed garbage disposal mechanism in the area, people carelessly dump garbage into rivers. Besides, the area's agricultural activity takes place on river banks and floodplains, and most of the boreholes are located in these areas, so the higher the Cd content in the area's surface water could be due to Cd from waste and phosphate fertilizers because Cd has a strong affinity for organic matter. Sometimes Cd can form minerals such as CdS,  $\text{CdCO}_3$  and CdO when Cd is associated with Zn and replaces Zn in sphalerite ( $\text{ZnS}$ ), galena ( $\text{PbS}$ ) and smithsonite ( $\text{ZnCO}_3$ ). Since Cd has a strong chalcophilic affinity, its mobility in sulfate- and carbonate-rich sediments at pH values below 8 is high as it forms complexity (Ladenberger et al. 2013).

The Pb content was measured between 0.003 mg/l and 0.078 mg/l and the mean was 0.044 mg/l (Fig. 3). 88.9% of water samples exceed the acceptable limit set by the WHO (0.01 mg/l) (Table 5). Higher Pb values were measured in samples from metavolcanic/clastic areas, suggesting that the source of Pb in this area may be lead-bearing minerals in these rocks (Beheemalingswara and Nata 2009).

The Cr concentration was measured between 0.001 mg/l and 0.08 mg/l, with a mean of 0.035 mg/l (Fig. 3). 22.2% of water samples exceed the WHO permissible limit (0.05 mg/l), while all water samples exceed the USEPA (2018) permissible limit (0.1 mg/l) (Table 5). Cr is moderately correlated with Cu and Cd, shows that the source Cr in the area could be metavolcanic/clastic rocks and anthropogenic activities.

The Zn content was measured between 0.538 mg/l and 1.18 mg/l, with a mean of 0.786 mg/l (Table 5, Fig. 3). There is no WHO health-based guideline for Zn, but tolerance above 4 mg/l may decrease. As a result, all water samples fell between the allowable ranges set by the WHO and USEPA.

Ni levels were measured between 0.012 mg/l and 1.05 mg/l, with a mean of 0.449 mg/l, and 61.1% of water samples above the permissible limit set by the WHO (Table 5, Fig. 3). The source of this metal in the region's water may be Ni-bearing minerals from metavolcanic/clastic rocks.

Generally, it can be inferred that contaminants like organic compounds introduced through human activities can elevate the release of Fe and Mn from aquifer sediments into groundwater, thereby exacerbating groundwater pollution by these metals (Zhai et al. 2021). Elevated levels of Cu, Pb and Zn in sediment are likely linked to sewage discharge (anthropogenic activities) from residential and industrial sources (Fabián et al. 2013). Therefore, the high concentration of the heavy metals in the study area could be resulted from both geogenic and anthropogenic processes.

To study the distributions of the heavy metal concentrations, three spatial distribution maps of Fe, Cu and Ni were developed. The resulting map shows that the north-west, southwest and southeast parts of the study have higher groundwater pollution with respect to metal contaminants (Fig. 4). Lineaments played an important role in the distribution of heavy metal concentrations and the central part of the study area, where lineaments are rarely observed, shows a lower concentration than the west and southwest parts (Fig. 4a, b).

## Heavy metal pollution assessment

The results of the pollution assessment indices are shown in the Table 6. HPI values were between 91.8 and 3408.6 with a mean of 1100.3. The HPI findings revealed that 94.4% of the water samples were exceeded the permissible limit of 100 suggested by Prasad and Bose (2001) for drinking. Only one sample was within the critical value (Table 6).

The HEI values in this case were between 9.7 and 70.2 (Table 6). Only one of the eighteen water samples, SBH11, had an HEI below 10 is regarded as low pollution. Surface water sample (SW2) is the type of water sample that provided the higher value. Anthropogenic and partially geogenic sources of heavy metals because surface waters to have a comparatively higher heavy metal content than borehole water.

As indicated in Table 6, the water samples degree of contamination (Cd) values varied from 0.7 to 61.2. Only one sample had a value below 1, indicating a low pollution level by Edet and Offiong's (2002) classification.

## Health risk assessment

The calculated chronic daily index (HI) value of metals for both adults and children shows that all water samples are higher for noncarcinogenic health risks ( $\text{HI} > 1$ ) (Tables 7

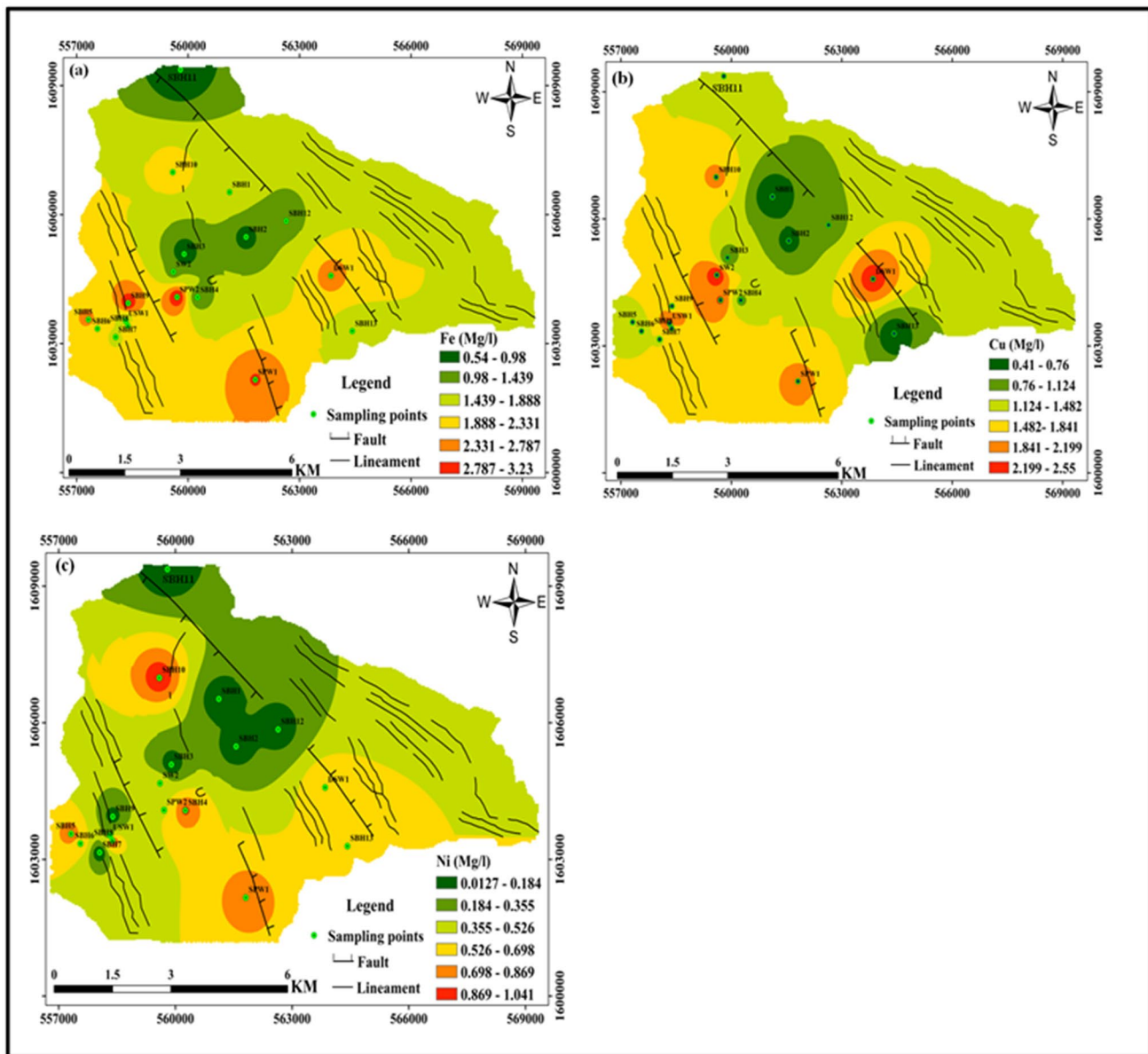


**Fig. 4** Spatial distribution maps of Fe (a), Cu (b) and Ni (c) of the study area. The northwest, southwest and southeast parts show a higher groundwater pollution with respect to metal contaminants

and 8). It is suggested that the local population faces health risk to noncarcinogenic. The HQ in the study area was detected in the order of  $Cd > Pb > Co > Cu$  for both adults and children. These metals made a greater contribution to the higher value of HI according to their order. In all the water samples, Cd made a greater contribution to the higher HI values for both adults and children. The HI value results also indicated that children are more at risk than adults to these potential health hazards (Tables 7; Fig. 5). A higher HI value for water from surface water (SW2 and DSW1) and SBH10 from groundwater for adults and children were calculated, and these wells are located along the lineament

orientation (Figs. 2, 5). This reveals that the lineaments have impact on aquifer leakage from rainfall or wastewaters.

For carcinogenic health risks, CR for Ni was detected to be higher in all water samples. All the water samples had CR values above the recommended range ( $CR > 1 \times 10^{-4}$ ) for Ni, both for adults and children. 88.9% of the water samples showed that a CR value above the recommended value ( $CR > 1 \times 10^{-4}$ ) for Cd and Cr, for both adult and children. Only two water samples (SBH9, SBH11) for Cd and SBH1 and SBH11 for Cr showed within the recommended risk standard for adults and children (Table 8). Generally, the result indicates that the local population the area is faced

**Table 6** Pollution evaluation indices of domestic water supply sources

Water sample	Sample code	HPI	HEI	Cd
Borehole water	SBH1	314	35.1	26
	SBH2	473	32.3	23
	SBH3	1151.5	29.9	20.9
	SBH4	360	40.3	31.3
	SBH5	771.5	43.6	34
	SBH6	1568.8	53.3	44.3
	SBH7	1428.5	34.7	25.7
	SBH8	1492	55.6	46.6
	SBH9	190	29.9	20
	SBH10	2324.9	67.7	58.8
	SBH11	111.3	9.7	0.7
	SBH12	91.8	21	12
	SBH13	605	41.6	32.6
Spring water	SPW1	613	37.3	28.3
	SPW2	1592.2	53.4	44.5
Surface water	USW1	1523.9	34.8	25.8
	DSW1	1784.71	51.4	42.4
	SW2	3408.6	70.2	61.2

with the carcinogenic health problems. The accumulated Cd concentration in the human body may cause harm to the kidneys, liver, testicles, lungs and hematopoietic system (Tinkov et al. 2018). Ni can have a number of negative health impacts on people, including the renal illness, lung cancer and heart failure (Genchi et al. 2020). A high intake of Cr in water may cause liver and kidney damage; it may also affect a man's sperm count and cause babies to grow more slowly than expected (Lopez et al. 2021).

## Multivariate statistical source appraisal of heavy metals

### Correlation analysis

The possible correlation between these trace metals, and two physicochemical parameter (EC and TDS) were determined using a Pearson correlation matrix. It is a useful method to determine whether the trace metals come from natural or anthropogenic activities (Islam et al. 2023). As shown in Table 9, the Pearson correlation matrix, some of the heavy metals have a significant but moderate correlation ( $p < 0.05$ ), highlighted in bold. Copper (Cu) has moderately positive relationships with Cd ( $r = 0.705$ ) and Cr ( $r = 0.642$ ). There is also a strong to moderate negative correlation with Mn ( $r = -0.894$ ) and Co ( $r = -0.633$ ) ( $p < 0.01$ ). Cd has a significant, moderately positive correlation with Cr ( $r = 0.612$ ) and Cu ( $r = -0.705$ ). Cd has also a moderate negative correlation with Mn ( $r = -5.76$ ), TDS ( $r = -0.74$ ) and EC ( $r = -0.734$ ).

Manganese shows a moderate positive correlation with Co ( $r = 0.756$ ). Fe also shows a weak positive correlation with Ni ( $r = 0.399$ ) and Pb shows a weak positive correlation with Zn ( $r = 0.346$ ). The positive relationship of the heavy metals suggests the same geogenic or anthropogenic sources. Nevertheless, in this study, geological processes are the dominant source of these heavy metals, while there is a possibility of an anthropogenic source for some heavy metals like Cd and Cu. Conversely, a strong negative correlation between the elements indicates probably different sources.

### Principal component analysis

Multivariate statistical analysis supports in determining the sources of pollution and identifies the primary determinants influencing groundwater quality (Egbueri and Unigwe 2020). One of the multivariate statistical methods that preserve the inherent details of the original set of data while minimizing the dimension of the data set to a smaller number of principal components is principal component analysis (Ganiyu et al. 2021). In many environmental analysis studies, PCA has been extensively used to validate Pearson correlation analysis results (Egbueri and Unigwe 2020).

The Kaiser–Meyer–Olkin (KMO) test is a measure of how suited your data is for Factor Analysis. The test measures sampling adequacy for each variable in the model and for the complete model (Watkins 2018). The Kaiser–Meyer–Olkin (KMO) is  $> 0.5$ , and the significance value is 0.00, as shown in Table 10, indicating that the study's data are appropriate for PCA. In order to obtain specific parameters and data that the correlation analysis was unable to capture, PCA was employed in this study. Table 11 presents a summary of the factors' rotated component matrix along with each factor's cumulative percent, percent of variance and eigenvalue.

Performing PCA, four components with Eigen values greater than one were taken out, and the loading map of the three most significant factors from the PCA is presented in Fig. 6. High positive contributions from Cu (0.905), Cd (0.527) and Cr (0.598) and high negative contributions from Mn (-0.902) and Co (-0.788) contributed to factor 1, which explained 40.68% of the variance. Factor 1 showed that both anthropogenic and natural processes are the sources of these elements.

A higher concentration of Cd and Cr in surface water close to towns and agricultural areas could be a result of agricultural practices like phosphate fertilizer use and inappropriate waste disposal. Negative loading of Co and Mn can suggest that although the geological composition of the rocks is the primary source of these elements, human activity may also be a contributing factor.

With strong positive loading from TDS (0.904) and EC (0.965), factor 2 explained 15.384% of the variation.

**Table 7** Hazard quotient (HQ) and hazard index (HI) of heavy metals in groundwater and surface water sources for adult and children

Sample code	Fe	Mn	Co	Cu	Cd	Pb	Cr	Zn	Ni	$\sum$ HQ=HI
<i>Adults</i>										
SBH1	0.09	0.35	21.0	0.34	6.0	3.89	4E-05	$8 \times 10^{-2}$	0.145	31.89
SBH2	0.0395	0.284	9.03	0.546	8.0	7.185	0.0003	0.0783	0.152	25.32
SBH3	0.03	0.243	10.9	0.669	15.3	4.213	0.0008	0.077	0.093	31.6
DSW1	0.12	0.031	5.79	1.995	48.8	4.44	0.0009	0.077	1.12	62.4
SBH4	0.052	0.23	7.47	0.862	4.0	6.85	0.0011	0.064	1.503	21.03
SBH5	0.12	0.145	7.0	1.033	17.9	4.91	0.0008	0.096	1.32	32.5
SBH6	0.09	0.181	2.6	1.072	41.3	5.47	0.0013	0.131	1.085	51.9
SBH7	0.086	0.102	2.94	1.17	41.2	0.83	0.0006	0.059	0.02	46.4
SBH8	0.1091	0.16	7.53	1.27	41.1	1.481	0.001	0.077	1.745	53.4
USW1	0.058	0.036	5.73	2.09	43.1	2.44	0.0015	0.087	0.16	53.7
SBH9	0.154	0.16	6.36	1.45	0.67	5.944	0.0014	0.13	0.123	14.9
SBH10	0.103	0.14	5.87	1.604	64.7	3.315	0.0018	0.083	1.645	77.4
SPW1	0.134	0.063	3.92	1.603	14.0	4.203	0.0002	0.065	1.338	25.3
SPW2	0.1543	0.108	3.19	1.88	42.2	5.56	0.003	0.086	0.862	54.04
SW2	0.061	0.042	3.02	2.13	96.7	5.26	0.0016	0.1087	0.752	108.1
SBH11	0.026	0.077	4.06	1.12	2.67	0.278	2E-05	0.079	0.118	8.419
SBH12	0.062	0.225	5.69	0.84	0.8	1.111	0.0002	0.087	0.162	8.98
SBH13	0.079	0.232	9.27	0.467	12.0	6.2	0.0002	0.107	1.125	29.5
<i>Children</i>										
SBH1	0.18	0.7	42.2	0.678	10.0	8.019	8.9E-05	0.16	0.287	62.25
SBH2	0.0791	0.567	18.07	1.092	16.0	14.37	0.0007	0.157	0.303	50.64
SBH3	0.0543	0.486	21.84	1.338	30.7	8.43	0.0016	0.154	0.187	63.2
DSW1	0.238	0.063	11.58	3.99	97.6	8.889	0.0018	0.152	2.233	124.7
SBH4	0.1038	0.459	14.93	1.723	8.0	13.7	0.0021	0.129	3.007	42.1
SBH5	0.2391	0.291	14.0	2.067	35.7	9.815	0.0016	0.192	2.63	64.97
SBH6	0.18	0.361	5.20	2.143	82.53	10.94	0.0011	0.262	2.17	103.8
SBH7	0.1724	0.204	5.889	2.348	82.4	1.667	0.0012	0.1196	0.04	92.841
SBH8	0.218	0.321	15.07	2.546	82.13	2.963	0.002	0.1536	3.483	106.8
USW1	0.1162	0.072	11.47	4.173	86.13	4.889	0.003	0.174	0.32	107.3
SBH9	0.308	0.32	12.71	2.896	1.33	11.89	0.0027	0.2609	0.247	29.9
SBH10	0.206	0.277	11.73	3.208	129.3	6.629	0.0036	0.1649	3.29	154.8
SPW1	0.268	0.126	7.844	3.207	28.0	8.407	0.0003	0.1307	2.677	50.7
SPW2	0.309	0.23	6.46	3.753	84.4	11.13	0.002	0.1727	1.723	108.1
SW2	0.122	0.085	6.044	4.267	193.3	10.52	0.0032	0.2176	1.503	216.1
SBH11	0.051	0.154	8.111	2.237	5.33	0.556	4.4E-05	0.1589	0.2367	16.84
SBH12	0.125	0.45	11.38	1.687	1.6	2.22	0.0014	0.174	0.323	17.961
SBH13	0.1591	0.4657	18.533	0.9333	24.0	12.41	0.0003	0.214	2.25	58.963

Geologic processes are the source of TDS and EC, as indicated by this factor. More weight is placed on geologic sources of TDS and EC than man-made ones in the environment, though anthropogenic activity is also expected for the enrichment of these physicochemical parameters.

Factor three shows a strong positive loading contribution with Fe (0.73) and Ni (0.852) and with a total variance of 13.296. This suggests the source of these metals is the same which is geogenic source mainly the weathering of metavolcanic/clast rocks. Redox conditions affect iron, which is readily mobilized as  $\text{Fe}^{2+}$  in anoxic conditions.

Additionally, factor 4 possesses a strong positive loading of Zn (0.868) and lead (0.69), accounting for 9.796% of the variance. Factor 4 showed that geologic processes, resulting from the reduction of sulfide minerals are the source of Zn and Pb. As stated by many researchers who conducted research in low-grade basement rock-dominated areas throughout the world and particularly in Tigray, while highly sheared rocks in these rock types are good for groundwater potential, they are also sources of base metal sulfide minerals (Beheemalingswara and Nata 2009; Siraj 2022).

**Table 8** Cancer risk of heavy metals due to drinking water for adults and children

Sample code	Cancer risk (Adults)				Cancer risk (Children)			
	Cd	Pb	Cr	Ni	Cd	Pb	Cr	Ni
SBH1	9.5E-05	1.23E-05	3.33E-05	4.87 × 10 <sup>-3</sup>	1.9 × 10 <sup>-4</sup>	2.45E-05	6.67E-05	9.8 × 10 <sup>-3</sup>
SBH2	1.52 × 10 <sup>-4</sup>	2.19E-05	2.57 × 10 <sup>-4</sup>	5.16 × 10 <sup>-3</sup>	3.04 × 10 <sup>-4</sup>	4.39E-05	3.1 × 10 <sup>-4</sup>	1.03 × 10 <sup>-2</sup>
SBH3	2.91 × 10 <sup>-4</sup>	1.28E-05	6.17 × 10 <sup>-4</sup>	3.17 × 10 <sup>-3</sup>	5.83 × 10 <sup>-4</sup>	2.58E-05	1.23 × 10 <sup>-3</sup>	6.35 × 10 <sup>-3</sup>
DSW1	9.27 × 10 <sup>-4</sup>	1.36E-05	6.57 × 10 <sup>-4</sup>	3.79 × 10 <sup>-2</sup>	1.85 × 10 <sup>-3</sup>	2.72 × 10 <sup>-5</sup>	1.31 × 10 <sup>-3</sup>	7.59 × 10 <sup>-2</sup>
SBH4	7.6E-05	2.09E-05	8 × 10 <sup>-4</sup>	5.11 × 10 <sup>-2</sup>	1.52 × 10 <sup>-4</sup>	4.19E-05	1.6 × 10 <sup>-3</sup>	1.03 × 10 <sup>-1</sup>
SBH5	3.39 × 10 <sup>-4</sup>	1.50E-05	5.83 × 10 <sup>-4</sup>	4.47 × 10 <sup>-2</sup>	6.79 × 10 <sup>-4</sup>	3.00E-05	1.17 × 10 <sup>-3</sup>	8.94 × 10 <sup>-2</sup>
SBH6	7.84 × 10 <sup>-4</sup>	1.68E-05	4 × 10 <sup>-4</sup>	3.69 × 10 <sup>-2</sup>	1.57 × 10 <sup>-3</sup>	3.35E-05	8 × 10 <sup>-4</sup>	7.38 × 10 <sup>-2</sup>
SBH7	7.83 × 10 <sup>-4</sup>	2.55E-06	4.33 × 10 <sup>-4</sup>	6.8 × 10 <sup>-4</sup>	1.57 × 10 <sup>-3</sup>	5.1E-06	8.67 × 10 <sup>-4</sup>	1.36 × 10 <sup>-3</sup>
SBH8	7.80 × 10 <sup>-4</sup>	4.53E-06	7.5 × 10 <sup>-4</sup>	5.92 × 10 <sup>-2</sup>	1.56 × 10 <sup>-3</sup>	9.07E-06	1.5 × 10 <sup>-3</sup>	11.84 × 10 <sup>-2</sup>
USW1	8.18 × 10 <sup>-4</sup>	7.48E-06	1.13 × 10 <sup>-3</sup>	5.4 × 10 <sup>-3</sup>	1.64 × 10 <sup>-3</sup>	1.49E-05	2.27 × 10 <sup>-3</sup>	1.09 × 10 <sup>-2</sup>
SBH9	1.27E-05	1.82E-05	1.03 × 10 <sup>-3</sup>	4.19 × 10 <sup>-3</sup>	2.53E-05	3.64E-05	2.06 × 10 <sup>-3</sup>	8.39 × 10 <sup>-3</sup>
SBH10	1.23 × 10 <sup>-3</sup>	1.01E-05	1.34 × 10 <sup>-3</sup>	5.59 × 10 <sup>-2</sup>	2.46 × 10 <sup>-3</sup>	2.02E-05	2.68 × 10 <sup>-3</sup>	11.19 × 10 <sup>-2</sup>
SPW1	2.66 × 10 <sup>-4</sup>	1.29E-05	1.2 × 10 <sup>-4</sup>	4.55 × 10 <sup>-2</sup>	5.32 × 10 <sup>-4</sup>	2.57E-05	2.33 × 10 <sup>-4</sup>	9.1 × 10 <sup>-2</sup>
SPW2	8.02 × 10 <sup>-4</sup>	1.70E-05	7.5 × 10 <sup>-4</sup>	2.93 × 10 <sup>-2</sup>	1.60 × 10 <sup>-3</sup>	3.40E-05	1.5 × 10 <sup>-3</sup>	5.86 × 10 <sup>-2</sup>
SW2	1.84 × 10 <sup>-3</sup>	1.61E-05	1.20 × 10 <sup>-3</sup>	2.56 × 10 <sup>-2</sup>	3.67 × 10 <sup>-3</sup>	3.21E-05	2.40 × 10 <sup>-3</sup>	5.11 × 10 <sup>-2</sup>
SBH11	5.07E-05	8.50E-07	1.67E-05	4.02 × 10 <sup>-3</sup>	1.01 × 10 <sup>-4</sup>	1.7E-06	3.33E-05	8.05 × 10 <sup>-3</sup>
SBH12	1.52E-05	3.4E-06	5.33 × 10 <sup>-4</sup>	5.49 × 10 <sup>-3</sup>	3.04 × 10 <sup>-5</sup>	6.8E-06	1.07 × 10 <sup>-3</sup>	1.09 × 10 <sup>-2</sup>
SBH13	2.28 × 10 <sup>-4</sup>	1.89E-05	1.17 × 10 <sup>-4</sup>	3.83 × 10 <sup>-2</sup>	4.56 × 10 <sup>-4</sup>	3.79E-05	2.33 × 10 <sup>-4</sup>	7.65 × 10 <sup>-2</sup>

**Fig. 5** Hazard index (HI) of adults and children in water sources, indicating a higher HI value for water from surface water (SW2, DSW1) and SBH10 from groundwater for adults and children

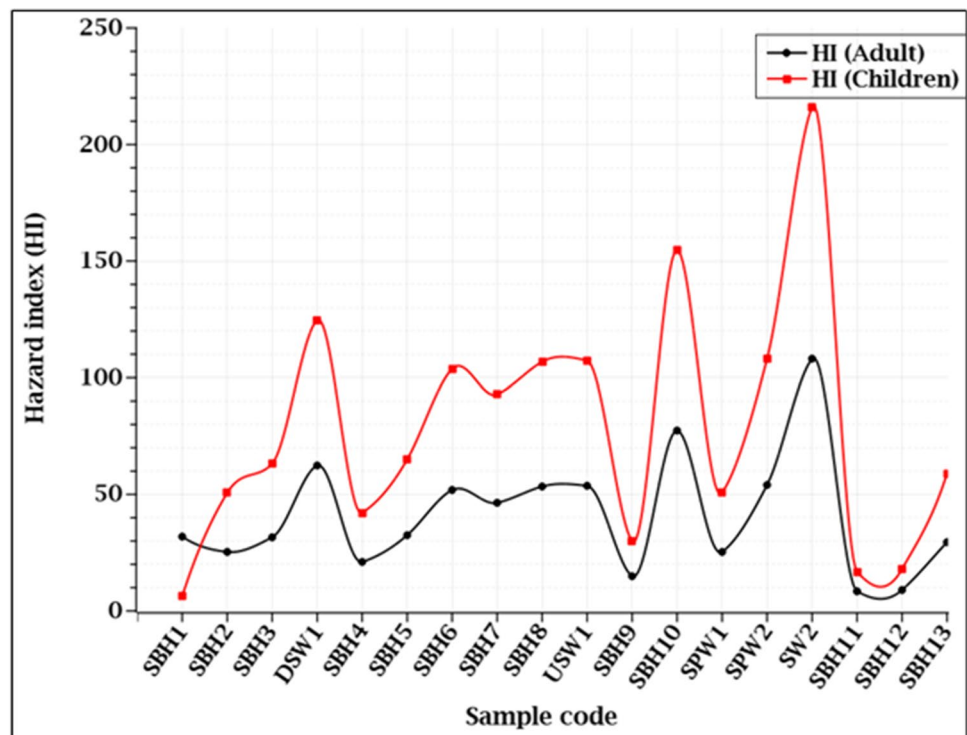


**Table 9** Pearson correlation matrix

Parameters	Fe	Mn	Co	Cu	Cd	Pb	Cr	Zn	Ni	TDS	EC
Fe	1										
Mn	-.258	1									
Co	-.160	.756**	1								
Cu	.391	-.894**	-.633**	1							
Cd	.129	-.576*	-.422	.705**	1						
Pb	.179	.307	.152	-.120	-.050	1					
Cr	.180	-.385	-.322	.642**	.612**	.073	1				
Zn	.227	.024	-.143	.075	.120	.364	.210	1			
Ni	.399	-.171	-.197	.203	.307	.237	.224	-.036	1		
TDS	-.106	.409	.339	-.420	-.740**	.117	-.263	-.079	-.277	1	
EC	-.096	.371	.287	-.394	-.734**	.093	-.242	-.075	-.257	.997**	1

\*\*Correlation is significant at the 0.01 level (2-tailed)

\*Correlation is significant at the 0.05 level (2-tailed)

**Cluster analysis**

Cluster analysis is a technique for performing classification by grouping variables according to their similarity. To capture the cluster distance, HCA with the squared

**Table 10** KMO and Bartlett’s test

Kaiser–Meyer–Olkin measurement of sampling adequacy	0.52
Bartlett’s test of sphericity	Approximate. Chi-square
	76.205
	df
	36
	Sig
	0.00

**Table 11** Rotated component matrix of three factors model<sup>a</sup>

Parameters	Components			
	1	2	3	4
Fe	.288	.080	.730	.181
Mn	-.902	.206	-.091	.201
Co	-.788	.136	-.055	.029
Cu	.905	-.244	.182	.034
Cd	.527	-.732	.092	.125
Pb	-.281	.060	.387	.693
Cr	.598	-.220	.098	.367
Zn	.123	-.039	-.073	.868
Ni	.046	-.259	.852	-.044
TDS	-.207	.954	-.074	.022
EC	-.163	.965	-.066	.011
Eigen value	4.475	1.692	1.463	1.078
% of total variance	40.680	15.384	13.296	9.796
% of cumulative variance	40.680	56.064	69.360	79.156

Extraction method: principal component analysis

Rotation method: varimax with kaiser normalization

<sup>a</sup>Rotation converged in 5 iterations

Euclidean distance Wards linkage method was used in this study. Three groups were created, as shown in the dendrogram in Fig. 7. The first group consists of Cd, Cr, Co, Mn and Pb, this combination suggests that the source for these elements is the same, which is possibly a geogenic source. Co and Mn are compatible in many Mg–Fe silicate minerals and have a strong metallic affinity for iron in the liquid phase. Cd and Cr metals are also compatible and lithophile elements. Cu, Zn, Ni and Fe are also belonging to the second group. Due to their strong affinity and similar geochemical behaviors, these metals commonly occur together in various natural settings. These metals are commonly found together in sulfide mineral deposits such as chalcopyrite (CuFeS<sub>2</sub>), sphalerite (ZnS) and pyrite (FeS<sub>2</sub>). These metals can be formed due to hydrothermal processes. Since Fe and Ni metals are compatible

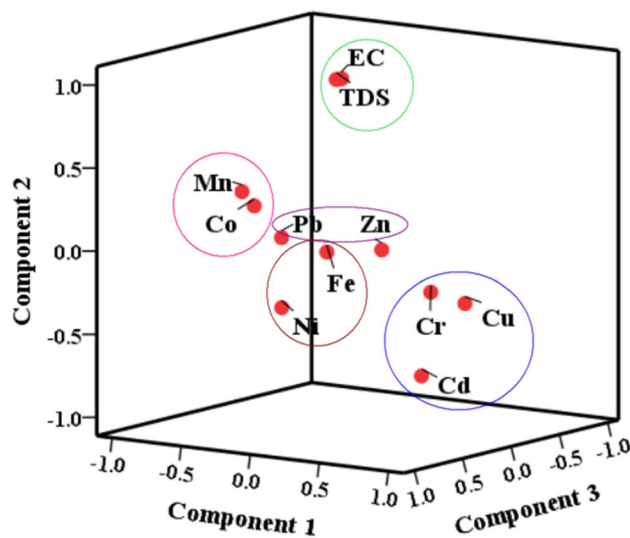
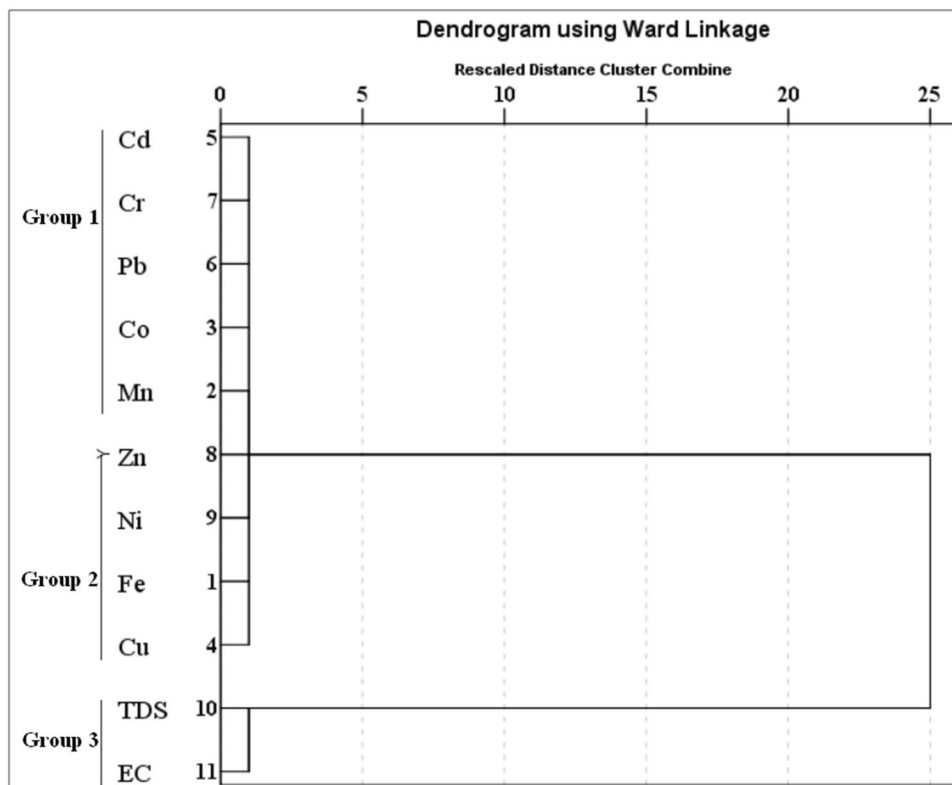


**Fig. 6** Component plot in rotated space

**Fig. 7** Hierarchical cluster analysis of heavy metals



components in the Mg–Fe silicate minerals and siderophile (iron lovers), they are geogenic sourced.

The study area is predominantly covered by metavolcanic and metasediment rocks. Since Cd forms complexity and can be found in sulfate and carbonate-rich sediments at pH values lower than 8. The high concentration of Cd in some surface water samples is probably caused by anthropogenic activity, such as the use of phosphate fertilizers in agriculture and the generation of municipal waste from towns, even though geogenic sources account for the majority of the region's Cd supply. The third group comprises the physicochemical parameters, EC and TDS. This reveals those two parameters affect each other as the dissolution of ions and metals increase in water. The discovery of numerous shear zones characterizes the study area. Hand-dug wells and shallow wells were built in shear zones because they are good potential aquifers. However, base metal mineralization (Cu, Fe, Mn and Pb) and associated metals (Co, Cd, Ni and Cr) can occur in these shear zones (Beheemalingswara and Nata 2009).

### Conclusions

The present study is concerned with assessing the degree of contamination with heavy metals in water resources, the comprehensive contamination level of metals, health risks

and the possible cause heavy metal contamination in mountain-bounded and low-grade basement rock-dominated areas of the Irob catchment.

The groundwater and surface water resources of the study area are subalkaline to alkaline in nature. The WHO has not established a health-based guideline for electrical conductivity and total dissolved solids, but a higher EC and TDS value may reduce the suitability of water for drinking if the EC value is > 1500  $\mu\text{s}/\text{cm}$  and TDS > 1000 mg/l. Accordingly, EC > 1500  $\mu\text{s}/\text{cm}$  and TDS > 1000 mg/l were found in 38.9% and 46.67% of the water samples, respectively.

The analyzed water samples revealed that 100% of the samples were over the WHO allowable limit for Fe and Mn, 88.9% for Pb, 83.5% for Cd, 55.5% for Cu, 50% for Ni and 5.6% for Co. The HEI and HPI showed that 94.4% of the water samples had a higher level of heavy metal contamination. Moreover, the  $C_d$  value of heavy metals showed a higher level of contamination. These three indices indicate that the area's groundwater, and surface water resources are not suitable for consumption.

The hazard index (HI) of metals for adults and children showed that ( $HI > 1$ ). Likewise, 88.9% of the water samples showed a cancer risk value above the recommended value ( $CR > 1 \times 10^{-4}$ ) for Cd and Cr for both adults and children.

According to the results of principal component analysis (PCA), cluster analysis (CA) and multivariate statistical analysis, human activities (solid and liquid waste disposals,

and fertilizer for agriculture) and natural processes (rock and soil weathering) are responsible for controlling the presence of heavy metals in the groundwater and surface waters of the area).

This study suggests that to protect public health and stop additional pollution of aquifers and surface water, contaminated groundwater and surface water resources should be routinely monitored and treated before being used by the relevant agency or stakeholders.

**Acknowledgements** The authors thank to Mekelle University for the research support. The IIE Scholar Rescue Fund and Jackson School of Geosciences are acknowledged for supporting Tewodros Alemayehu's research stay at the University of Texas at Austin.

**Funding** The first author received a research grant from Mekelle University and it is acknowledged in the acknowledgement statement.

## Declarations

**Conflict of interest** On the behalf of the authors, I would like to declare that we have no known competing financial interests or personal relationships that could have appeared to influence the work reported in this paper.

**Open Access** This article is licensed under a Creative Commons Attribution-NonCommercial-NoDerivatives 4.0 International License, which permits any non-commercial use, sharing, distribution and reproduction in any medium or format, as long as you give appropriate credit to the original author(s) and the source, provide a link to the Creative Commons licence, and indicate if you modified the licensed material. You do not have permission under this licence to share adapted material derived from this article or parts of it. The images or other third party material in this article are included in the article's Creative Commons licence, unless indicated otherwise in a credit line to the material. If material is not included in the article's Creative Commons licence and your intended use is not permitted by statutory regulation or exceeds the permitted use, you will need to obtain permission directly from the copyright holder. To view a copy of this licence, visit <http://creativecommons.org/licenses/by-nc-nd/4.0/>.

## References

- Abraham M, Dereje F, Berihu A (2024) multivariate and water quality index approaches for spatial water quality assessment in Lake Ziway. *Ethiopian Rift Water Air Soil Pollut* 235:78
- Ahamad A, Raju NJ, Madhav S, Khan AH (2020) Trace elements contamination in groundwater and associated human health risk in the industrial region of southern Sonbhadra Uttar Pradesh India. *Environ Geochem Health* 42:3373–3391
- Ahmed S, Akhtar N, Rahman A, Mondal NC, Khurshid S, Sarah S, Kamboj V (2022) Evaluating groundwater pollution with emphasizing heavy metal hotspots in an urbanized alluvium watershed of Yamuna River Northern India. *Environ Nanotechnol Monit Manag* 18:100744
- Alemu CM, Aycheh YF, Angualie GS, Engidayehu SS (2024) Modeling on comprehensive evaluation of groundwater quality status using geographic information system (GIS) and water quality index (WQI): a case study of Bahir Dar City, Amhara. *Ethiopia Water Pract Technol* 19(4):1084–1098
- Alene M, Jenkin GR, Leng MJ, Darbyshire DF (2006) The tambien group Ethiopia: an early Cryogenian (ca 800–735 Ma) neoproterozoic sequence in the Arabian-Nubian shield. *Precambrian Res* 147(1–2):79–99
- APHA (2017) Standard methods for the examination of water and waste water, 22nd edn. American Public Health Association Water Environment Federation, Washington
- Aschale M, Yilma S, Mary K, Dereje H (2011) Multivariate analysis of potentially toxic elements in surface waters in Ethiopia. *Appl Water Sci* 11:1–13
- Barrie CT, Abdalla MAF, Hamer RD (2016) Volcanogenic massive sulphide–oxide gold deposits of the Nubian Shield in Northeast Africa. In: Bouabdellah M, Slack JF (eds) *Mineral Deposits of North Africa*. Springer International Publishing, Cham
- Berhea S, Letab S (2015) Suitability assessment of water quality of assabol dam for irrigation fish culture and drinking purposes at erob wereda eastern Tigray; Ethiopia
- Bheemalingeswara K, Tadesse N (2009) Petrographic and geochemical study of low grade metamorphic rocks around Negash with reference to base metal mineralization and groundwater quality Tigray northern Ethiopia. *Momona Ethiopian J Sci* 1(2):106–132
- Björklund G, Skalny AV, Rahman MM, Dadar M, Yassa HA, Aaseth J, Tinkov AA (2018) Toxic metal (loid)-based pollutants and their possible role in autism spectrum disorder. *Environ Res* 166:234–250
- Brown E, Skougstad MW, & Fishman MJ (1970) Methods for collection and analysis of water samples for dissolved minerals and gases (No. 05-A1). US Govt. Print
- Chiamsathit C, Auttamana S, Thammarakcharoen S (2020) Heavy metal pollution index for assessment of seasonal groundwater supply quality in hillside area Kalasin Thailand. *Appl Water Sci* 10(6):1–8
- De Putter T, Mees F, Decrée S, Dewaele S (2010) Malachite an indicator of major Pliocene Cu remobilization in a karstic environment (Katanga Democratic Republic of Congo). *Ore Geol Rev* 38(1–2):90–100
- Dey M, Akter A, Dey IS, Choudhury SC, Fatema TR, Begum KJ, BA, (2021) Assessment of contamination level pollution risk and source apportionment of heavy metals in the Halda River water Bangladesh. *Heliyon* 7(12):e08625
- Edet AE, Offiong OE (2002) Evaluation of water quality pollution indices for heavy metal contamination monitoring. A study case from Akpabuyo-Odukpani area lower cross river basin (southeastern Nigeria). *GeoJournal* 57:295–304
- Edokpayi JN, Enitan AM, Mutileni N, Odiyo JO (2018) Evaluation of water quality and human risk assessment due to heavy metals in groundwater around Muledane area of Vhembe District Limpopo Province South Africa. *Chem Cent J* 12:1–16
- Egbueri JC (2020) Heavy metals pollution source identification and probabilistic health risk assessment of shallow groundwater in Onitsha Nigeria. *Anal Lett* 53(10):1620–1638
- Fabián FL, Fernando LV, Prócoro GM, Silvia LS, Elsa NAG, Arturo IM, del María SGG, Gildardo HM, Raúl HM, Manuel AÁG, Ixchel RPV (2013) Heavy metal pollution in drinking water—a global risk for human health: a review. *Afr J Environ Sci Technol* 7(7):567–584
- Ganiyu SA, Oyadeyi AT, Adeyemi AA (2021) Assessment of heavy metals contamination and associated risks in shallow groundwater sources from three different residential areas within Ibadan metropolis southwest Nigeria. *Appl Water Sci* 11(5):81
- Gebreyohannes GW (2014) Geology geochemistry and geochronology of Neoproterozoic rocks in western Shire Northern Ethiopia. MSc Dissertation, University of Oslo



- Genchi G, Sinicropi MS, Lauria G, Carocci A, Catalano A (2020) The effects of cadmium toxicity. *Int J Environ Res Public Health* 17(11):3782
- Hagos M, Gebreyohannes T, Amare K, Hussien A, Berhane G, Walraevens K, Cavalazzi B (2020) Tectonic link between the Neoproterozoic dextral shear fabrics and Cenozoic extension structures of the Mekelle basin Northern Ethiopia. *Int J Earth Sci* 109:1957–1974
- Haile TA, Tewodros A, Berhe BA (2024) Hydrogeochemical characterization of groundwater in mountainous catchment and its suitability for drinking purposes in Irob, Tigray. *Northern Ethiopia Water Pract Technol* 19(4):1495–1512
- Hakanson L (1980) An ecological risk index for aquatic pollution control. A Sedim Logical Approach *Water Res* 14(8):975–1001
- Hayelom DB, Gebregziabher BB (2015) The level of heavy metals in potable water in Dowhan Erop Wereda Tigray Ethiopia. *J Nat Sci Res* 3(1):190–194
- Islam MS, Hossain MK, Phoungthong K, Ismail Z, Othman IK, Ishak DSM, Idris AM (2023) Heavy metals in soil of three agroforestry systems: a preliminary study for source identification and ecological risk. *Int J Environ Anal Chem* 11:1–17
- Jamshaid M, Arshad AK, Kashif A, Monawwar S (2018) Heavy metal in drinking water its effect on human health and its treatment techniques—a review. *Int J Biosci* 12(4):223–240
- Kaiser HF (1958) The varimax criterion for analytic rotation in factor analysis. *Psychometrika* 23(3):187–200
- Kawo NS, Karuppannan S (2018) Groundwater quality assessment using water quality index and GIS technique in Modjo River Basin, central Ethiopia. *J Afr Earth Sc* 147:300–311
- Kebede NM, Ambushe AA, Bhagwan SC, Mesfin RA, McCrindle RI (2012) Potentially toxic elements in some fresh water bodies in Ethiopia. *Toxicol Environ Chem* 94(10):1980–1994
- Khelfaoui M, Benaissa A, Kherraf S, Madjram MS, Bouras I, Mehri K (2022) Assessment of groundwater and surface water pollution by hazardous metals using multivariate analysis and metal pollution index around the old Sidi Kamber mine NE Algeria. *Pollution* 8(3):889–903
- Kumar V, Sharma A, Kumar R, Bhardwaj R, Kumar Thukral A, Rodrigo-Comino J (2020) Assessment of heavy-metal pollution in three different Indian water bodies by combination of multivariate analysis and water pollution indices. *Hum Ecol Risk Assess Int J* 26(1):1–16
- Kwaansa-Ansah EE, Nti SO, Opoku F (2019) Heavy metals concentration and human health risk assessment in seven commercial fish species from Asafo Market Ghana. *Food Sci Biotechnol* 28(2):569–579
- Ladenberger A, Andersson M, Reimann C, Tarvainen T, Filzmoser P, Uhlbäck J, Sadeghi M (2013) Geochemical mapping of agricultural soils and grazing land (GEMAS) in Norway Finland and Sweden—regional report. Geological Survey of Sweden Uppsala
- Li P, Karunanidhi D, Subramani T, Srinivasamoorthy K (2021) Sources and consequences of groundwater contamination. *Arch Environ Contam Toxicol* 80:1–10
- López-Botella A, Velasco I, Acién M, Sáez-Espinosa P, Todolí-Torró JL, Sánchez-Romero R, Gómez-Torres MJ (2021) Impact of heavy metals on human male fertility an overview. *Antioxidants* 10(9):1473
- Mebrahtu G, Zerabruk S (2011) Concentration of heavy metals in drinking water from urban areas of the Tigray region northern Ethiopia. *Momona Ethiopian J Sci* 3(1):105–121
- Melaku S, Wondimu T, Dams R, Moens L (2004) Simultaneous determination of trace elements in Tinishu Akaki River water sample, Ethiopia, by ICP-MS. *Can J Anal Sci Spectrosc* 49(6):374–384
- Mineral resource reviews. Springer International Publishing, Switzerland, PP 417–435
- Mohamed SB (2022) Geochemical and petrological survey in Northern Ethiopia basement rocks for investigation of gold and base metal mineralization in finarwa area and its surrounding southeast zone of Tigray Ethiopia. *American J Geospat Technol* 1(1):15–28
- Prasad B, Bose J (2001) Evaluation of the heavy metal pollution index for surface and spring water near a limestone mining area of the lower Himalayas. *Environ Geol* 41(1–2):183–188
- Prasanna MV, Praveena SM, Chidambaram S, Nagarajan R, Elayaraja A (2012) Evaluation of water quality pollution indices for heavy metal contamination monitoring: a case study from Curtin Lake Miri City East Malaysia. *Environ Earth Sci* 67:1987–2001
- Ren X, Li P, He X, Su F, Elumalai V (2021) Hydrogeochemical processes affecting groundwater chemistry in the central part of the Guanzhong Basin China. *Arch Environ Contam Toxicol* 80:74–91
- Sadeghi M, Morris GA, Carranza EJM, Ladenberger A, Andersson M (2013) Rare earth element distribution and mineralization in Sweden: an application of principal component analysis to FOREGS soil geochemistry. *J Geochem Explor* 133:160–175
- Tabor M, Kibret M, Abera B (2011) Bacteriological and physicochemical quality of drinking water and hygiene-sanitation practices of the consumers in Bahir Dar city, Ethiopia. *Ethiopian j health sci* 21(1):19–26
- Teym A, Mengistie E, Tiku S, Fekadu S, Berihun G, Ahmednur M, Negesse A (2021) Determination of heavy metal contamination in ground and surface water sources in Jimma Town, Southwest Ethiopia. *J Environ Pollut Human Health* 9(2):36–43
- Tong S, Li H, Tudi M, Yuan X, Yang L (2021) Comparison of characteristics water quality and health risk assessment of trace elements in surface water and groundwater in China. *Ecotoxicol Environ Safety* 219:112283
- UNICEF (2019) Progress on drinking water sanitation and hygiene 2000–2017. *Special focus on inequalities*
- USEPA (1998) National recommended water quality criteria. *Fed Reg* 63(234):67548–67558
- USEPA IRIS (2011) Integrated risk information system. Environmental protection agency region I, Washington, p 20460
- USEPA (2018) Regulation Development for Drinking Water Contaminants. National Primary Drinking Water Regulations and National Secondary Drinking Water Regulations. U.S. Environmental Protection Agency Washington DC USA.
- Virág L, Erdodi F, Gergely P (2016) Bioinorganic chemistry for medical students. *Scriptum University of Debrecen, Hungary*, pp 1–104
- Wagh VM, Panaskar DB, Mukate SV, Gaikwad SK, Muley AA, Varade AM (2018) Health risk assessment of heavy metal contamination in groundwater of Kadava River Basin Nashik India. *Modeling Earth Syst Environ* 4:969–980
- Wang WuJ, Wang Y, Ji Y (2020) Finding high-quality groundwater resources to reduce the hydatidosis incidence in the Shiqu County of Sichuan Province China: analysis assessment and management. *Expo and Health* 12:307–322
- Wang L, Li P, Duan R, He X (2022) Occurrence controlling factors and health risks of Cr 6+ in groundwater in the Guanzhong Basin of China. *Expo and Health* 14:239–251
- Watkins MW (2018) Exploratory factor analysis: a guide to best practice. *J Black Psychol* 44(3):219–246
- Wei M, Pan A, Ma R, Wang H (2023) Distribution characteristics source analysis and health risk assessment of heavy metals in farmland soil in Shiquan County Shaanxi Province. *Process Saf Environ Prot* 171:225–237
- WHO (2022) Guidelines for drinking-water quality: incorporating the first and second addenda. World Health Organization, Switzerland

- Xiao J, Wang L, Deng L, Jin Z (2019) Characteristics sources water quality and health risk assessment of trace elements in river water and well water in the Chinese Loess Plateau. *Sci Total Environ* 650:2004–2012
- Yousefi M, Ghoochani M, Mahvi AH (2018) Health risk assessment to fluoride in drinking water of rural residents living in the Poldasht city Northwest of Iran. *Ecotoxicol Environ Saf* 148:426–430
- Zhai Y, Han Y, Xia X, Li X, Lu H, Teng Y, Wang J (2021) Anthropogenic organic pollutants in groundwater increase releases of Fe and

Mn from aquifer sediments: impacts of pollution degree, mineral content, and pH. *Water* 13:1920

**Publisher's Note** Springer Nature remains neutral with regard to jurisdictional claims in published maps and institutional affiliations.